Scientific paper

The Role of Specific Interaction in Phase Behavior of Polyelectrolyte-Surfactant-Water Mixtures

Simona Sitar,[1] Bart Goderis,[2] Per Hansson[3] and Ksenija Kogej[1,*]

[1] *Department of Chemistry and Biochemistry, Faculty of Chemistry and Chemical Technology, University of Ljubljana, Aškerčeva 5, PO Box 537, SI-1000 Ljubljana, Slovenia.*

[2] *Molecular and Nanomaterials, Department of Chemistry, Catholic University of Leuven, Celestijnenlaan 200F, B-3001 Heverlee, Belgium.*

[3] *Department of Pharmacy, Biomedical Centre, Uppsala University, Box 580, SE-75123 Uppsala, Sweden.*

** Corresponding author: E-mail: ksenija.kogej@fkkt.uni-lj.si*
Tel.: +(386-1)-2419-412; Fax: +(386-1)-2419-425

Received: 09-01-2012

Dedicated to Prof. Dr. Gorazd Vesnaver on the occasion of his 70th birthday

Abstract

Aqueous phase behavior and structures of phases were studied in systems containing sodium poly(styrenesulfonate), NaPSS, and complex salt CTAPSS, formed between cetyltrimethylammonium cations, CTA^+, and PSS^- anions. It was shown that hydrophobic interaction of the polyion styrene groups with surfactant aggregates, which supports the strong electrostatic attraction between CTA^+ and PSS^-, has a significant effect on phase behavior and structures. Only the disordered micellar (L_1) and the ordered hexagonal (H_1) phase were found that are connected over a broad two-phase region of L_1-H_1 coexistence. At water contents above 60 wt%, CTAPSS is easily dissolved in proportion to the amount of added NaPSS, whereas at lower water contents a large excess of NaPSS is needed to dissolve CTAPSS. Phase separation in the two-phase region is controlled by two tendencies: (i) to maximize the contact between the hydrophobic groups and micelles (assisted by hydrophobic interaction) and (ii) to form as dense phase as possible (assisted by both, electrostatic and hydrophobic interactions). Structural characteristics of soluble non-stoichiometric complexes from the L_1 phase show that hydrophobic interaction contributes also to a relatively small size of PSS-induced micelles and leads to a network-like association between PSS chains in which micelles serve as cross-links.

Keywords: Polyelectrolyte-surfactant complexes, phase behavior, electrostatic interactions, hydrophobic interactions, hexagonal structure, micellar phase

1. Introduction

Strong association between oppositely charged polyions and surfactant ions in aqueous solutions often leads to phase separation.[1–3] The most common in these systems is the *associative* type of phase separation, upon which a concentrated phase of a polyelectrolyte-surfactant complex, PSC, is formed that is in equilibrium with a dilute solution containing excess low molar mass ions. These ions originate from the polyelectrolyte and the surfactant salt. The main driving force for PSC formation in the case of charged components is thus a large entropy increase associated with counterion release. Phase separation in polymer-surfactant mixtures can also be of a *segregative* type, upon which two phases are formed with very different content of components. The latter type is more commonly encountered in the case of uncharged or similarly charged components due to their mutual incompatibility, but can take place also in mixtures of oppositely charged species in the presence of sufficient amounts of added low molecular weight inert salt.[3] These two types of phase separation were described many years ago for mixed polymer solutions[4] and were shown to be appropriate also for the description of phase behavior in polymer-surfactant mixtures.[1,3]

The concentrated phases that separate out of polyelectrolyte-surfactant mixtures can be highly ordered, depending on structural features of the components involved, e.g. on surfactant chain length and polyion charge density, and on solvent environment, in particular on salt concentration. The presence of the polyion offers strong bridging attraction between polyion-induced micelles, which leads to a decrease in intermicellar distances and to further ordering. Small-angle X-ray scattering studies show that surfactant ions form a disordered phase of roughly spherical polyion-bound micelles at low surfactant-to-polyelectrolyte charge ratios,[5] whereas close to the 1:1 charge ratio liquid crystalline phases can be formed that exhibit long-range order. Structures of these phases range from cubic[6–11] to hexagonal[9,10,12,13] and lamellar.[9]

In this contribution we are interested in PSCs formed between poly(styrenesulfonate anion), PSS, and cationic surfactants. Salts of PSS (the most frequently used is its sodium salt, NaPSS) are strong polyelectrolytes with hydrophobic benzene groups in the chain carrying the charged sulfonate groups. The hydrophobic character of PSS side groups has no significant effect on its solution behavior, but turns out to be very important in its interactions with surfactants. It has been shown by NMR[14] that benzenesulfonate groups of PSS integrate into the hydrophobic interior of surfactant aggregates, close to their surface, which presents an additional attractive interaction and results in PSCs that are resistant to changing the external conditions, e.g. ionic strength,[15] or to exposing the soluble (non-stoichiometric) PSC to dynamic processes, e.g.direct current measurements.[15,16] It has been also established that the hydrophobic interaction strongly reduces surfactant aggregation number, N_{agg}, in comparison with that of free micelles.[17] Moreover, N_{agg} values in PSS solutions are not constant but increase with increasing surfactant content.[17]

Strong electrostatic interactions reinforced by the underlined specific hydrophobic attraction result in very strong binding of cationic surfactants by PSS.[18–21] On first thought, this should lead to phase separation (precipitation) of the PSC already at low surfactant-to-polyelectrolyte charge ratios. However, light scattering studies in dilute solutions show[15] that PSS-surfactant systems remain homogeneous one-phase solutions even when most (around 70%) of the charged sulfonate groups on PSS have been neutralized by surfactant ions, irrespective of salt concentration.[15,22] This is in sharp contrast with the case of surfactant mixtures involving sodium poly(acrylate), NaPA.[13] It was observed in that case that precipitation of a concentrated phase, containing the complex, starts already at very low additions of a cationic surfactant like cetyltrimethylammonium bromide, CTAB, to dilute NaPA solutions. PSS and PA are both vinyl-based polyions with the same structural value of the linear charge density parameter, but differ in their hydrophobic character. The completely ionized PA anion is an intrinsically hydrophilic polyion, for which no "mixed" polymer-surfactant aggregates can be formed, whereas PSS, through incorporation of its hydrophobic groups into micelle interior, forms some kind of mixed micelles with cationic surfactants.

We were interested in how this distinctive feature of PSS affects phase behavior of PSCs and in this frame also how it contributes to the solubility of the complex. We have prepared complex salt, denoted as CTAPSS, of PSS with a frequently investigated surfactant cation cetyltrimethylammonium, CTA^+, and studied its mixtures with NaPSS in H_2O. These mixtures correspond to polyelectrolyte-rich regime or to so-called polyion mixing plane in a three-dimensional presentation of phase diagrams in polyelectrolyte-surfactant-water mixtures.[23] The idea of using complex salts as the starting point in studying phase behavior of polyelectrolyte-surfactant systems was first introduced by Piculell and co-workers[7,8,24,25] in phase studies involving PA in order to reduce the number of components in such mixtures by eliminating counterions of either the polyelectrolyte or the surfactant salt. In CTAPSS/NaPSS/H_2O mixtures the surfactant counterion (e.g. Cl^-) is removed. Basically this means that low molar mass salt, which would be formed upon mixing polyion and surfactant-ion salts, is absent, and this greatly simplifies the interpretation of phase behavior. In order to construct the phase diagram, coexisting phases were separated and analyzed for compositions and structures. Structures were determined by small-angle X-ray scattering, SAXS.

2.Experimental

2. 1. Materials and Methods

2. 1. 1. Materials

Sodium poly(styrenesulfonate), NaPSS, with a nominal molecular weight of 70.000 g/mol (corresponding to around 340 monomer units) and a degree of sulfonation 1.0, supplied by Polysciences Inc., Warrington, PA, was used as the starting material. NaPSS was converted to poly(styrenesulfonic acid), HPSS, by dialysis against HCl. Afterwards, HPSS was purified by dialysis against Millipore water and ultrafiltration and finally concentrated by vacuum distillation. The concentration of HPSS stock solution was determined by neutralization potentiometric titration. Cetyltrimethylammonium chloride, CTAC, was purchased from Fluka Analytical and was used as received.

2. 1. 2. Preparation of the Complex Salt

The complex salt CTAPSS was prepared by following the previously proposed procedures,[6] i.e. by titrating the hydroxide form of the surfactant, cetyltrimethylammonium hydroxide, CTAOH, with HPSS. The first step was to convert CTAC to CTAOH by ion exchange. The

ion-exchange resin, Dowex MTO SRB LCM G Supelco, was charged by stirring it in excess amount of 1 M NaOH for 2 hours and then rinsed with distilled water until the rinsing water reached pH ≈ 7. CTAC (7 g) was dissolved in a plastic beaker containing a large excess (150 mg) of resin and 100 ml of distilled water. The solution was stirred for 2 hours, filtered, and the filtrate was rinsed with distilled water into a new batch of 150 mg of resin and 100 ml of water. This mixture was then stirred for another 2 hours. The last step was repeated once more with a third fresh batch of resin. The final product was an alkaline solution of CTAOH. The absence of Cl^- ions in this solution was proven by the reaction with $AgNO_3$. The freshly prepared solution of CTAOH was titrated drop by drop into the HPSS stock solution under vigorous stirring. The titration was continued until the equivalence point was reached, upon which a white precipitate was formed in solution. The equivalence point (pH = 7.05) was determined from a separate pH titration curve obtained by titrating HPSS with CTAOH.

After equilibrating overnight the solution with the precipitate was freeze-dried for several days up to a constant weight. The complex salt was obtained as a white and very light compound, which was put to storage over silica gel in a desiccator. Elemental analysis confirmed a 1:1 molar ratio between CTA^+ and SO_3^- groups in the CTAPSS complex.

2. 1. 3. Sample Preparation

First, samples of CTAPSS and water were prepared by weighing calculated amounts of substances into glass tubes. Samples were mixed for a short time with a vortex vibrator and then centrifuged for 15 minutes in the centrifuge at 4000 rpm. Afterwards, the tubes were flame-sealed and left to stand at 40 °C overnight. The next day, mixing by centrifugation was continued during 5 hours with turning the tubes end over end every 30 minutes. The samples were then kept in an oven at 40 °C for 10 days. After 10 days they were centrifuged again for a short time without turning them around. The entire procedure of heating, centrifugation, and turning of samples is needed to facilitate inter-diffusion of components, in particular in dense systems with low water content where PSS chains, since they are rather long, diffuse slowly. Samples prepared in this way were left to equilibrate at 25 °C for 3 to 6 months, depending on sample viscosity and appearance.

In addition to CTAPSS/H_2O mixtures, samples of the complex salt, water, and polyelectrolyte (NaPSS) were prepared as well. Again, appropriate amounts of CTAPSS, NaPSS and water were weighted into glass tubes. The mixing procedure was the same as described above. Water content in binary samples (CTAPSS/H_2O mixtures) was between 30 and 98 wt%, whereas in ternary mixtures (CTAPSS/NaPSS/H_2O mixtures) it was above 40 wt%.

2. 1. 4. Determination of Structures and Compositions of Equilibrium Phases

The characterization of samples was first carried out by visual inspection in normal light and through crossed polarizers to detect eventual presence of optically anisotropic phases and then more precisely by SAXS. SAXS measurements were conducted using two SAXS setups: the synchrotron small-angle X-ray scattering at the Dutch-Belgian Beamline BM26B of the European Synchrotron Radiation Facility (ESRF) in Grenoble and a high performance SAXS instrument "SAXSess" from Anton Paar KG, Graz, Austria. The block-collimating unit of the latter system was attached to a conventional X-ray generator (Philips, Holland) equipped with a sealed X-ray tube (Cu anode target type producing Cu Kα X-rays with a wavelength, λ, of 0.154 nm) operating at 35 kV and 35 mA. The scattered X-ray intensities were measured with a linear position sensitive detector. Liquid-like samples were filled in capillaries, whereas for dense phases, special sample holders for pastes and powders SWAXS from Hecus were used. The synchrotron experiments were executed at λ = 0.775 Å. A 2D multiwire gas-filled detector was placed at 1.5 m from the sample after an evacuated tube. The reflections of a silver behenate standard were used to calibrate the scattering angles,[26] expressed as a function of q, with $q = 4\pi\sin\theta/\lambda$ and θ being half of the scattering angle. Data were accumulated at room temperature for 60 s with the samples being presented in a rubber ring, sandwiched between thin mica sheets. The sandwich construction was kept together in an aluminum frame which ensures a sample thickness of 1 mm. The SAXS patterns were normalized to the intensity of the incoming beam, measured by an ionization chamber placed downstream from the sample, and corrected for the detector response prior to azimuthally averaging the isotropic data using the homemade software ConeX.[27] Finally, the patterns were corrected for the scattering due to the empty setup, taking into account the sample and sample holder transmission.

The phase-separated samples from the two-phase regions were analyzed for compositions. For the determination of water content in separated phases the Karl-Fischer method was used. The concentration of PSS anion in liquid phases was determined by measuring the absorbance of UV light with a wavelength of 261.5 nm, and the concentration of Cl^- ions in liquid phases was assessed by potentiometric titration using $AgNO_3$ as a titrant.

2. 1. 5. Presentation of Results

Crucial for structural properties and PSC solubility is the mole fraction of sodium ions in mixtures that arise from the gradual addition of NaPSS to the CTAPSS complex salt. The addition of NaPSS leads to the formation of non-stoichiometric complex solutions, denoted as (Na, CTA)PSS, where one part of the polyion charge is blocked by large and polyion-immobilized CTA^+ micelles and

the other one is screened by small and mobile Na^+ ions. We define the mole fraction of sodium ions, X_{Na+}, in the counterion population of the PSS anion in these complexes as

$$X_{Na^+} = \frac{n_{Na^+}}{n_{Na^+} + n_{CTA^+}} \quad (1)$$

Because CTA^+ is completely bound by the polyion in the form of micelles, X_{CTA+} (= $1 - X_{Na+}$) represents the fraction of charged groups on the polyion that are neutralized/blocked[16] by surfactant aggregates, and X_{Na+} corresponds to the fraction of "free" charges. This type of binding was proven previously by measuring various thermodynamic and transport properties[16,28] in solutions of PSS anion and cetylpyridinium cations. Note that sodium ions bind electrostatically to the highly charged polyion, thus reducing its charge density to an effective value, while they retain a considerable part of their mobility along the polyion chain.

Alternatively, parameter f can be introduced to characterize the complexes as the molar ratio between negative charges ensuing from styrenesulfonate (SS^-) groups and positive charges arising from CTA^+:

$$f = \frac{n_{SS^-}}{n_{CTA^+}} \quad (2)$$

Here, n_{SS^-} and n_{CTA+} are moles of styrene sulfonate, SS^-, and CTA^+ groups in (Na,CTA)PSS mixtures, respectively. It is to be noted that f equals $(X_{CTA+})^{-1}$, since $n_{SS^-} = n_{Na+} + n_{CTA+}$ due to electro-neutrality condition. Thus, upon NaPSS addition to CTAPSS the value of f increases from 1 ($X_{CTA+} = 1$) for pure CTAPSS complex salt (the case with no excess negative charge) to infinity ($X_{CTA+} = 0$) for pure NaPSS (only Na^+ ions present).

3. Results and Discussion

3. 1. Phase Diagram

Phase diagram showing progression of structures in CTAPSS/NaPSS/H_2O mixtures is presented in Figure 1 as a plot of X_{Na+} (or f, see right axis) versus water content given in weight % (wt%). Only two phases were identified: a disordered micellar, L_1, phase at high water content (above approximately 60 wt% of H_2O) and an ordered hexagonal, H_1, phase at low water content (below 40–45 wt% of H_2O). The homogeneous hexagonal phase extends over the whole range of X_{Na+} values, whereas the micellar phase appears for $X_{Na+} > 0.3$ ($f > 1.4$). At water content around 60 wt%, the micellar phase is stable even down to $X_{Na+} \approx 0.1$ ($f \approx 1.1$). It is worthwhile to stress that no cubic phase was detected in CTAPSS/NaPSS/H_2O mixtures.

The transformation of L_1 to H_1 takes place over a broad two-phase region where both phases coexist. For $X_{Na+} > 0.3$ (or $f > 1.4$) this is between 45 and 60 wt% H_2O, whereas for lower X_{Na+} the two-phase region broadens along the $X_{Na+} = 0$ axis all up to almost 100 wt% H_2O. Note that samples with $X_{Na+} = 0$ correspond to binary mixtures of stoichiometric CTAPSS complex and water (c.f. samples marked by filled triangles in Figure 1 on the $X_{Na+} = 0$ axis). The hexagonal phase in binary CTAPSS/H_2O mixtures swells up to around 43 wt% of water. For higher water content, it separates into a complex-rich hexagonal phase and virtually pure water.

SAXS pattern of the one-phase CTAPSS sample with 31 wt% of H_2O is shown in Figure 2a and clearly displays a strong first order hexagonal peak at $q \approx 1.54$ nm^{-1} and additional higher order peaks that fit the characteristic sequence 1: √3: √4: √7 for the H_1 phase, which is composed of closed packed surfactant cylinders.

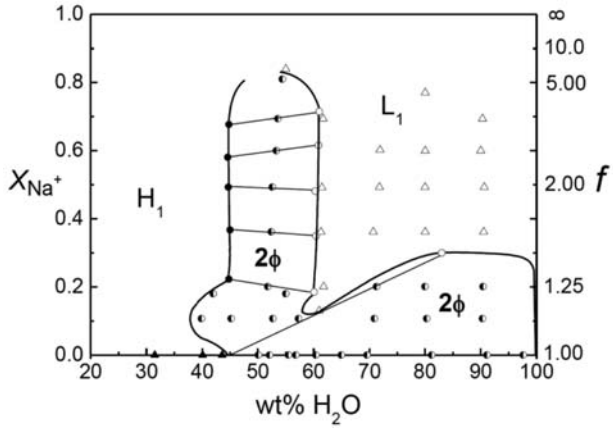

Figure 1. Phase diagram in CTAPSS/NaPSS/H_2O mixtures. One-phase samples are indicated by open (micellar or L_1 phase) and full (hexagonal or H_1 phase) triangles, two-phase samples by half-filled circles, and tie lines connect the equilibrium micellar (open circles) and hexagonal phase (full circles).

Different phase separation behaviors were observed in the irregularly shaped two-phase region, depending on water content. In the part close to the CTAPSS-H_2O axis with wt% $H_2O > 60$, the hexagonal phase is the dense (bottom) phase and the upper phase is a disordered micellar solution of a non-stoichiometric (Na,CTA)PSS complex with $X_{Na+} \approx 0.3$ (or $f \approx 1.4$). The coexisting phases are indicated by the tie line for a sample with $X_{Na+} = 0.2$ and 70 wt% of H_2O, which suggests that CTAPSS is solubilized in proportion to the amount of added NaPSS in such a way that a disordered solution of soluble (Na,CTA)PSS complex with $f \approx 1.4$ (excess of negative charge) is formed, whereas the non-solubilized part is the dense precipitate of CTAPSS with $f \approx 1$ (virtually no overall charge). This means that phases with $1 < f < 1.4$ are largely absent in this part of the phase diagram, whereas mixtures with $f > 1.4$ are completely soluble.

The described situation in CTAPSS/NaPSS/H_2O system is in sharp contrast with closely related mixtures involving PA (CTAPA/NaPA/H_2O).[25] In the following comparison, long PA chains are considered,[25] parallel to

relatively long PSS chains from this study (see Experimental Section). In long chain PA case, phases with any *f* were found as long as water content was high (above 95 wt%) and increasing the amount of NaPA in the system led to a gradual increase of *f* in the complex phase. The difference between the systems is also very clearly seen from the perspective of adding complex salts to pure polyelectrolyte solutions. While typically very small amounts of CTAPA can be added to NaPA solutions (with more than 95wt% of H_2O) without the separation out of a CTAPA rich phase, CTAPSS is completely dissolved in NaPSS solutions of any concentration as long as $f > 1.4$.

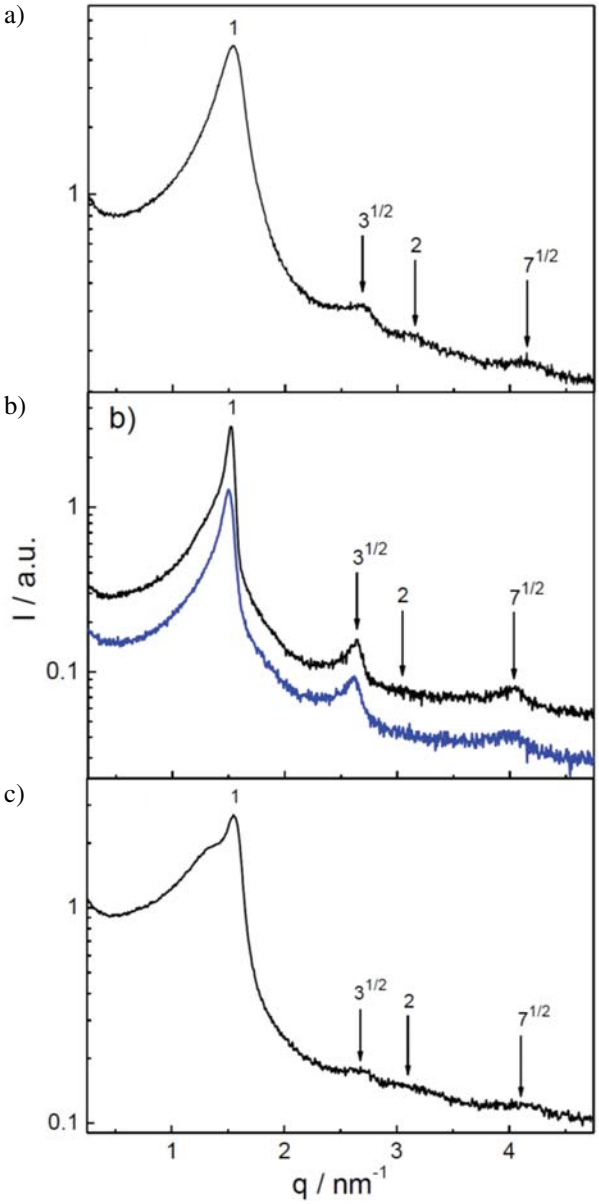

Figure 2. SAXS patterns of the hexagonal phase in a) a binary CTAPSS/H_2O mixture with 31 wt% of water and in b) two ternary CTAPSS/NaPSS/H_2O mixtures from the two-phase region with an overall amount of water around 50 wt% and $X_{Na+} = 0.5$ (black curve) and 0.2 (blue curve), and c) SAXS pattern of a sample with 42 wt% H_2O and $X_{Na+} \approx 0.2$ from the transitional region (see text). Arrows indicate peak positions.

The other part of the L_1-H_1 two-phase region extends up to $X_{Na+} \approx 0.82$ (or $f \approx 5.6$) and is located in the wt% H_2O range 45–60. It is characterized by a density inversion: here the upper phase (lighter) is the hexagonal one with lower water content and the bottom phase (heavier) is the disordered micellar phase. Phases with any *f* are possible in this region. The coexisting phases have about the same X_{Na+} (or *f*) values, indicated by the direction of tie lines for several samples from this region that are more or less parallel to the x-axis. This suggests that the system tends to conserve *f*. We believe that this tendency to preserve *f* is imposed by the hydrophobic interaction between the styrene groups and the hydrocarbon core of micelles. On the account of this, there is a strong affinity of the PSS backbone to incorporate into micellar interior, which was evidenced by NMR measurements.[14] An increase in *f* in either L_1 or H_1 phase would lead to a decrease in the contact between PSS hydrophobic groups and micelles, i.e. to an increase in their exposure to polar water environment, which is unfavorable. Instead, at any *f*, a dense phase that separates out tends to conserve *f* in order to minimize the hydrophobic energy. This feature is evidently absent in the NaPA case. Another important point in comparing PA and PSS systems is the N_{agg} values. In comparison with pure surfactant solutions, these are unchanged (and constant) in the presence of PA but strongly reduced (and dependent on *f*) in the presence of PSS. Smaller N_{agg}, and for this reason different packing conditions, may lead to a less efficient screening of the micellar charge by the polyion chain in the PSS case and therefore to a better solubility of the CTAPSS complex, which is experimentally observed. This point will be further discussed below.

Structure of the hexagonal phase in CTAPSS/NaPSS/H_2O mixtures is very similar to the one in binary CTAPSS/H_2O mixtures, as can be appreciated from the SAXS patterns of samples with $X_{Na+} = 0.49$ and 0.20 in Figure 2b. The position of the main hexagonal peak is found at the same *q* value as in stoichiometric complexes, i.e. at $q = (1.5–1.54)$ nm^{-1}, almost irrespective of X_{Na+}, and additional higher order peaks are clearly discernible.

The transition between both parts of the two-phase region was observed in the range 40 < wt% H_2O < 50 and for $X_{Na+} \approx 0.1–0.2$. In this region, the relative change in density (density inversion; see above) takes place. Both phase (L_1 and H_1) assume very similar density values and consequently separation of phases was impossible to achieve. Scattering patterns of these conglomerates displayed a broad micellar peak at $q \approx 1.35$ nm^{-1} and a superimposed hexagonal pattern with the main peak at $q \approx 1.55$ nm^{-1}, which is close to previously reported values. An example of such SAXS spectrum is shown in Figure 2c.

One can argue that the described phase behavior reflects two, partly conflicting, strives of the system: (1) to form a dense complex phase (favored by electrostatic inte-

ractions) and (2) to maximize the contact between PSS and micelles (favored by hydrophobic interactions). In principle, one solution to the problem would be to pack all of NaPSS and CTAPSS into one dense phase in equilibrium with pure water. In the frequently used triangular presentation of phase diagrams in three component systems, such two-phase region would appear as a droplet suspended from the water corner.[3,23] The reason why this is not realized in practice is probably that the attractive forces cannot balance the resulting strong swelling pressure due to the ions in the dense phase.

Under the influence of (2), on the other hand, the system tends to avoid phase separation if not all resulting phases get similar *f* values. In order to obtain osmotic balance between the phases, and still maintain the tendency to conserve *f* the two-phase region must shrink. This is observed in both, CTAPA/NaPA/H_2O[25] and CTAPSS/NaPSS/H_2O mixtures studied here, with an important difference that the L_1-H_1 two-phase region in the PSS case is broader in comparison with PA since it is promoted also by the hydrophobic interaction. In principle, when *f* approaches unity and the average net charge of the complexes is low, the two-phase region should broaden again, as is observed also experimentally (c.f. the broadening of the two-phase region along $X_{Na+} = 0$). If the driving force for associative phase separation dominates, the result should depend on the tendency of the complex phase to swell.

A remaining question is the absence of the cubic phase. One of the reasons that no cubic phase was detected could be the relatively long PSS chains used in our study (around 340 monomer units). Piculell and coworkers found a cubic phase with short PA chains (30 monomer units) but not with long ones (6000 monomer units).[25] Another very probable motive for the absence of the cubic phase is the solubilization of benzene groups in PSS-induced micelles. In dilute solutions (water content above 60 wt%) it is comparatively easy to bury hydrophobic rings into the surface of spherical micelles in the micellar phase. However, as the solute concentration increases and more and more PSS chains accumulate in the system, it becomes increasingly more difficult to achieve this with highly curved spherical micelles, but it may be easier in a concentrated phase with surfactant packed in the form of cylinders. Cylindrical micelles, aggregates with lower curvature, can be packed closer together and thus provide a more effective protection of the hydrophobic benzene groups against the polar environment of water. It can be suggested that effective close packing of surfactant, which is in this case required also by the specific feature of the polyion, is consistent with cylindrical rather than with globular micelles.

3. 2. The Micellar One-phase Region

Our interest in the following is properties of soluble (Na,CTA)PSS complexes from the region of the disordered micellar phase. Examples of SAXS patterns for micellar samples with $X_{Na+} = 0.49$ and increasing water content and those for samples with 63 wt% H_2O and increasing X_{Na+} are given in Figures 3a and 3b, respectively. SAXS patterns for all samples display a well-defined and broad correlation peak at $q \approx 1.6$–1.7 nm^{-1} that is usually associated with the center-to-center distance, *d*, between adjacent polyion-bound micelles. The clearest micellar patterns were observed for solutions with wt% $H_2O \geq 70$ (Figure 3a). Furthermore, curves for samples with wt% $H_2O \approx 63$, which are located close to the phase border with the two-phase region, develop an additional strong peak at a lower *q* (≈ 1.3 nm^{-1}, c.f. also Figure 2c) that is superimposed on the first micellar peak (Figure 3b). In addition, a very broad shoulder can be traced in all curves in the *q*-range 2.8–4 nm^{-1}. This shoulder is more pronounced in samples with higher X_{CTA+} (lower X_{Na+}) and lower wt% of H_2O and its inexplicit nature suggests stronger fluctuations in characteristic distances, which are associated with it.

From the position of peak maxima in SAXS patterns, denoted on the *q*-scale as q_{max}, the center-to-center separation between micelles (distance *d*) in the L_1 phase was calculated by using the usual expression

$$d = \frac{2\pi}{q_{max}} \tag{3}$$

Similarly, for the hexagonal phase the center-to-center distance between cylinders can be obtained from

$$d = \frac{2}{\sqrt{3}}\frac{2\pi}{q_1} \tag{4}$$

where q_1 is the position of the first diffraction peak in the SAXS spectrum of the H_1 phase.

In Figure 4, *d*-values for the micellar phase are plotted in dependence on X_{Na+} (or *f*; see upper axis) and in Figure 5 in dependence on total weight fraction of H_2O (or weight fraction of solid, wt% solid; see upper axis) in samples with $X_{Na+} = 0.49$. Note that in the case of 63 wt% H_2O (SAXS patterns in Figure 3b) two *d*-values are given in Figure 5, one associated with the main peak at a lower *q* (≈ 1.3 nm^{-1}), and another one (c.f. symbol in brackets) corresponding to the superimposed higher *q* peak. The latter (lower) *d*-value agrees with the trend in *d*-values at higher water content. Besides, *d*-values for the coexisting micellar (L_1) and hexagonal (H_1) phase of the two-phase sample with the same overall X_{Na+} (= 0.49) are included. It can be seen that *d* in the L_1 phase decreases with increasing X_{Na+} (Figure 4) and also with decreasing amount of water in the system (Figure 5). In monophasic samples with 50 wt% of H_2O on the NaPSS-rich side ($X_{Na+} > 0.8$ or $f > 5$) it suddenly jumps to higher values. Similarly, it shows an abrupt increase as the two-phase region at wt% $H_2O \approx 62$ (or wt% solid ≈ 38) is entered. The second sudden increase in *d* is an indication of the $L_1 \rightarrow H_1$ phase transition. The increase in *d* in NaPSS-rich samples with 50 wt% H_2O may also be an indication of a different type

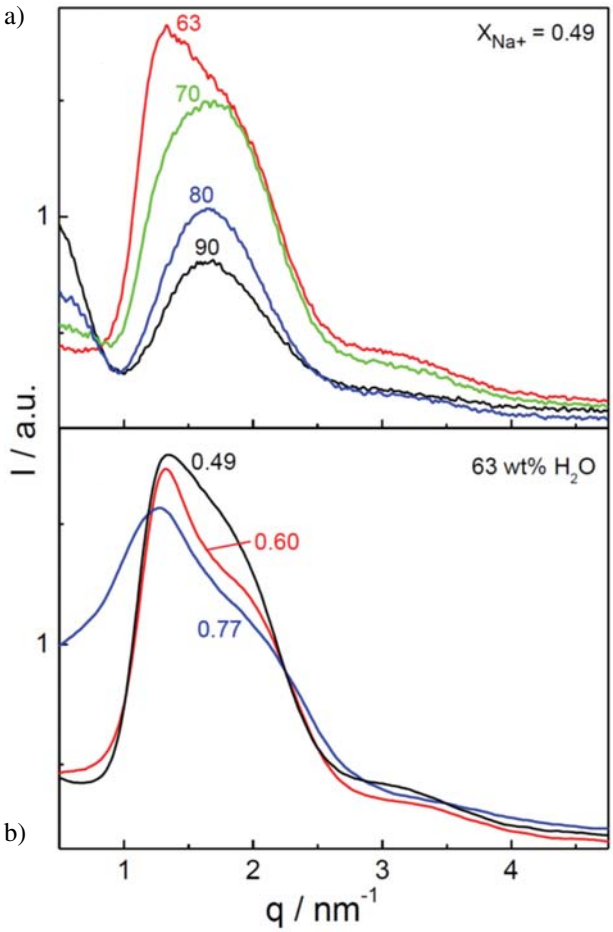

Figure 3. SAXS patterns of micellar samples a) with X_{Na+} = 0.49 and varying amounts of water (indicated in wt%-value associated with each curve) and b) with 63 wt% H_2O and varying X_{Na+} values (see numbers associated with each curve).

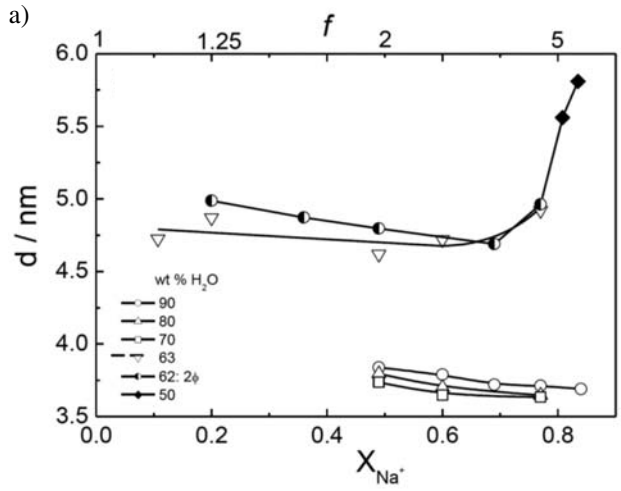

Figure 4. Values of characteristic distance *d* for micellar peaks of monophasic samples derived from SAXS patterns in dependence on X_{Na+}. Note that samples with 62 wt% H_2O designated by ◐ are biphasic (the data correspond to equilibrium micellar (L_1) phases) and those with 50 wt% H_2O and $X_{Na+} > 0.8$ are monophasic.

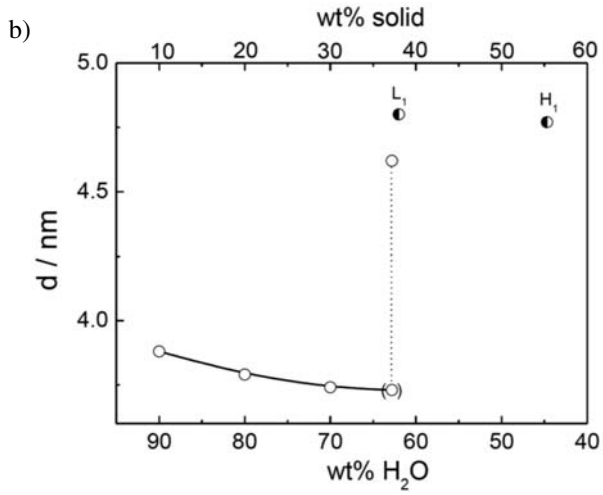

Figure 5. Characteristic distance *d* for micellar peaks of monophasic samples with X_{Na+} = 0.49 in dependence on wt% H_2O (or wt% solid; see upper axis). Samples with wt% $H_2O \leq 62$ designated by ◐ are biphasic; points show *d* for micellar (L_1) and hexagonal (H_1) peak.

of ordering (or loss of ordering) in systems that are rich in more or less free PSS chains. However, PSS solutions with low surfactant content ($f > 5$) were out of the scope of the present study and were not further investigated.

We first discuss samples that are situated well within the homogeneous L_1 phase (wt% $H_2O \geq 70$). In these solutions, *d* is between 3.60 and 3.95 nm (Figure 4) and does not depend much on solute concentration (i.e. on the total amount of H_2O). Based on the idea of a PSC in which polyion-induced micelles are bound to the chain next to each other,[16,17] these *d*-values should correspond to two surfactant hydrocarbon chain lengths (l_{C16} = 2.05 nm for a cetyl – C_{16} chain[29]), increased by the size of the ammonium head group (with a radius r_{NH4^+} = 0.175 nm) and by the thickness of the polyion chain that resides in the space between adjacent micelles (PSS radius is r_{PSS} = 0.8 nm[30]). Most likely, the last two contributions are smaller than suggested from dimensions of ions due to the described inclusion phenomenon. Still, experimental *d* values are evidently smaller than expected from these data and they are also smaller than values in comparable CTAPA/NaPA/H_2O mixtures.[8,21] It can be concluded that the presence of the PSS anion, through inclusion of its hydrophobic groups into the micelle, compresses the micelles. Additional effect of such binding is that the micellar aggregation number is reduced, as has been established by time-resolved fluorescence quenching measurements for CTAB micelles in the presence of PSS,[31] and this also contributes to a lower *d* value. It was demonstrated[31] that at high *f* (large PSS excess), N_{agg} is considerably lower than in pure surfactant solutions in water and it increases with decreasing *f* (i.e. with increasing amount of surfactant in complexes). For example, at $f \approx 4.8$ N_{agg} is around 33 and at $f \approx 1.5$ it is around 80, whereas for pure CTAB in water ($f = 0$) $N_{agg} \approx 120$ is

found. It is worthwhile to note that PA has no effect on surfactant aggregation numbers; N_{agg} values are the same in mixed solutions with PA and in pure CTAB solutions.[21]

It is close at hand to seek explanation for the PSS system in the emphasized hydrophobic interaction between PSS and micelles,[14] which is held responsible for the described considerable reduction of surfactant aggregation numbers.[21,31] Reduction of N_{agg} is equivalent to an increase of the area per surfactant in the head group region of the micelle, a_0,[32] showing that binding of PSS to micelles increases the distance between the head groups. This can be thought of as a way for the system to allow as many SS^- groups as possible to bind to micelles or, alternatively, as the result of weaker attraction between surfactants in the surface region of the micelle since the polymer reduces the 'surface tension' of micelles. On the other hand, in complexes with f approaching 1 (the stoichiometric CTAPSS complex salt), a_0 is the smallest, which favors aggregates with lower curvature (e.g. cylinders).[32] Thus, PSS incorporation into micelles may explain also why there is no cubic phase in CTAPSS/NaPSS/H_2O mixtures, which is expected to precede the hexagonal phase. Cubic structure in PSCs is often of the Pm3n type,[5,7,9,11,21] composed of discrete slightly elongated micelles,[21] which are aggregates with higher curvature in comparison with cylindrical micelles in the H_1 phase.

SAXS patterns of the one-phase micellar samples with 63 wt% H_2O, reported in Figure 3b, deserve more discussion. These are the monophasic micellar samples that are situated next to the two-phase region (see Figure 1). As already noted, SAXS patterns for these samples exhibit a very broad shoulder extending from $q \approx 2.8$ nm^{-1} to $q \approx 4$ nm^{-1}, in addition to the well-pronounced micellar peak at $q \approx 1.3$ nm^{-1} superimposed on the peak at $q \approx 1.7$ nm^{-1}. The center of this shoulder can be traced at around two-times larger q in comparison with the peak at 1.7 nm^{-1}. The corresponding correlation distance ($d \approx 1.8$–1.9 nm) may be a consequence of intermolecular association between PSCs, which would lead to some kind of a network-like structure involving several PSS chains connected by surfactant micelles. Surfactant micelles may be regarded as cross-links in the network. It is expected that such network-like association is rather disordered and subjected to stronger fluctuations in inter-particle distances in comparison with the inter-particle distance between firmly bound PSS-induced micelles in the primary complex. Clearly, this sort of a loose structure leads to broader and less intensive correlation peaks. This interpretation is supported by an additional feature: the height of this broad peak increases with increasing amount of surfactant in the complexes (i.e. with increasing X_{CTA+}), since more cross-links (i.e. more surfactant micelles) reduce fluctuations in the network. The loose network-like association involving discrete micelles is ultimately transformed into a highly ordered hexagonal structure when the amount of water in the system is reduced below 62 wt%. As noted above, d-values (c.f. Figure 5) clearly reflect phase separation: they jump from around 3.7 nm (the value estimated for the L_1 phase at around 63 wt% of H_2O) to around 4.7–4.8 nm. Note that d for the L_1 phase with 62 wt% of H_2O is ~4.8 nm and the one for the equilibrium H_1 phase with 45 wt% of H_2O is ~4.77 nm.

The order imposed to the system by surfactant micelles is ultimately lost on the NaPSS-rich side for $X_{Na+} > 0.8$. The SAXS curve for a monophasic sample with $X_{Na+} = 0.84$ and 50 wt% H_2O is shown in Figure 6 and shows a very broad shoulder centered at around 1.09 nm^{-1} ($d \approx 5.8$ nm). For comparison, SAXS curve for the micellar phase of a biphasic sample with $X_{Na+} = 0.77$ and the same overall amount of water is included. The micellar phase itself contains around 62 wt% of water. The latter case still displays a well-pronounced peak as a consequence of micelle-micelle correlations, in contrast with the first one, where the order is almost lost.

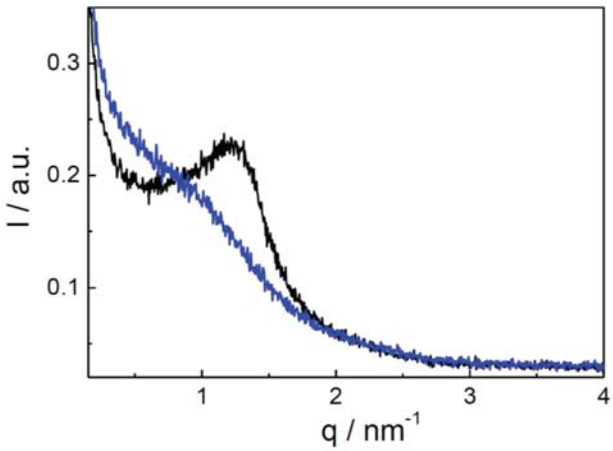

Figure 6. SAXS curve of a monophasic sample with $X_{Na+} = 0.84$ and 50 wt% H_2O (blue curve) and of a micellar phase of a biphasic sample with $X_{Na+} = 0.77$ and 62 wt% H_2O (black curve).

4. Conclusions

In this work, we have investigated phase behavior in mixtures of the complex salt formed between PSS anions and CTA^+ cations (designated as CTAPSS), NaPSS, and water. The system is characterized by a specific hydrophobic interaction between styrene groups of PSS and micelle interior that noticeably manifests itself in structural characteristic and in overall phase behavior. The major result is that this feature contributes to increased stability of the stoichiometric CTAPSS complex and may be one of the reasons for the absence of the cubic phase: only micellar and hexagonal phase appear in the phase diagram. Interestingly, the distinctive tendency to bind PSS to CTA^+ micelles, arising from inclusion of styrene groups into the surface region of micellar aggregates, promotes dissolution of CTAPSS by adding NaPSS. This can be explained by a less efficient screening of the overall micellar charge

by PSS anion arising from this specific interaction. This is the most evident difference in comparison with systems involving essentially hydrophilic polyions like PA.

In addition to two broad one phase regions (L_1 at wt% $H_2O > 60$ and H_1 at wt% $H_2O < 45$), a peculiarly shaped two phase region of $L_1 - H_1$ coexistence was identified, where phase separation follows two partly conflicting strives of the system: (1) to maximize the contact between hydrophobic SS groups and micelles and (2) to form a dense phase. Hydrophobic interaction plays a role in both efforts, albeit more significant in strive (1), and makes phase separation favorable only if the resulting phases obtain about the same *f*-values. Electrostatic interactions contribute mostly to aim (2), and, through involvement of hydrophobic interactions, lead to segregative-like phase separation of the system into an almost pure CTAPSS-H_2O phase ($f \approx 1$ and wt% $H_2O \approx 45$) and a phase of dissolved non-stoichiometric (Na,CTA)PSS complex with $f \approx 1.4$. Obviously, $f \approx 1.4$ or higher ($X_{Na+} = 0.3$ or higher) guarantees sufficient net charge of the solubilized non-stoichiometric complex to resist phase separation.

Structural characteristics of soluble (Na,CTA)PSS complexes from the disordered micellar phase also reveal the highlighted hydrophobic involvement of the polyion in aggregate formation, through which micellar aggregation numbers are considerably reduced. This is reflected in the rather low value of the inter-micellar spacing *d* deduced from SAXS patterns. The latter parameter decreases with increasing *f* (i.e. with increasing NaPSS content in complexes), since the intimate hydrophobic binding of PSS to the micelle increases the distance between head groups and thus also the head group area per surfactant monomer, which is consistent with a lower N_{agg}. SAXS patterns show that polyion-induced micelles, in particular at decreased water content in the system, serve as cross-links in a network of PSS chains.

5. Acknowledgments

This work was supported by the Slovenian Research Agency, ARRS, through the program Physical Chemistry P-0201. B. G. thanks FWO Vlaanderen for supporting the ESRF-DUBBLE, Big Science project. P. H. is thankful to the Swedish research council for financial support.

6. References

1. L. Piculell, B. Lindman, *Adv. Colloid Interf. Sci.* **1992**, *41*, 149–178.
2. B. Lindman, K. Thalberg, *Polymer-Surfactant Interactions – Recent Developments*; in *Interaction of Surfactants with Polymers and Proteins*; E. D. Goddard, K. P. Ananthapadmanabhan, Eds.; CRC Press: Boca Raton, Florida, 1993, Chapter 5.
3. L. Piculell, B. Lindman, G. Karlström, *Phase Behaviour of Polymer-Surfactant Systems*; in *Polymer-Surfactant Systems*; J. C. T. Kwak, Ed., Marcel Dekker, Inc.: New York, 1998, Chapter 3.
4. H. G. Bungeberg de Jong, in *Colloid Science* (H. R. Kuyt, Ed.), Elsevier, New York, Volume II, 1949, pp. 232–258.
5. K. Kogej, G. Evmenenko, E. Theunissen, H. Berghmans, H. Reynaers, *Langmuir* **2001**, *17*, 3175–3184.
6. P. Ilekti, T. Martin, B. Cabane, L. Piculell, *J. Phys. Chem.* **1999**, *103*, 9831–9840.
7. A. Svensson, L. Piculell, B. Cabane, P. Ilekti, *J. Phys. Chem. B* **2002**, *106*, 1013–1018.
8. A. Svensson, L. Piculell, L. Karlsson, B. Cabane, B. Jönsson, *J. Phys. Chem. B* **2003**, *107*, 8119–8130.
9. K. Kogej, G. Evmenenko, E. Theunissen, J. Škerjanc, H. Berghmans, H. Reynaers, W. Bras, *Macrom. Rapid Commun.* **2000**, *21*, 1226–1233.
10. K. Kogej, *Adv. Colloid Interf. Sci.* **2010**, *158*, 68–83.
11. K. Kogej, *J. Phys. Chem. B* **2003**, *107*, 8003–8010.
12. J. O. Carnali, *Langmuir* **1993**, *9*, 2933–2941.
13. P. Ilekti, L. Piculell, F. Tournilhac, B. Cabane, *J. Phys. Chem.* **1998**, *102*, 344–351.
14. Z.Gao, R. E. Wasylishen, J. C. T. Kwak, *J. Colloid Interface Sci*, **1988**, *126*, 371–376.
15. S. Prelesnik, S. Larin, V. Aseyev, H. Tenhu, K. Kogej, *J. Phys. Chem. B*, **2011**, *115*, 3793–3803.
16. J. Škerjanc, K. Kogej, in *Macroion Characterization. From Dilute Solutions to Complex Fluids*; K. S Schmitz, Ed.; ACS Symposium Series 548; American Chemical Society: Washington, DC, 1994; Chapter 20, pp 268–275.
17. M. Almgren, P. Hansson, E. Mukhtar, J. van Stam, *Langmuir*, **1992**, *8*, 2405–2412.
18. K. Kogej, J. Škerjanc, *Surfactant Binding to Polyelectrolytes*, in *Physical Chemistry of Polyelectrolytes*; T. Radeva, Ed.; Surfactant Science Series, vol. 99; Marcel Decker: New York, 2001; Chapter 21, pp 793–827.
19. J. Škerjanc, K. Kogej, G. Vesnaver, *Phys. Chem*, **1988**, *92*, 6382–6385.
20. K. Kogej, J. Škerjanc, *Langmuir* **1999**, 15, 4251–4258.
21. P. Hansson, M. Almgren, *Langmuir* **1994**, *10*, 2115–2124.
22. R. G.Nause, D. A. Hoagland, H. H. Strey, *Macromolecules* **2008**, *41*, 4012–4019.
23. K. Thalberg, B. Lindman, G. Karlstrom, *J. Phys. Chem.* **1991**, *95*, 6004–6011.
24. S. dos Santos, C. Gustavsson, C. Gudmundsson, P. Linse, L. Piculell, *Langmuir* **2011**, *27*, 592–603.
25. A. Svensson, J. Norrman, L. Piculell, *J. Phys. Chem. B* **2006**, *110*, 10332–10340.
26. T. C. Huang, H. Toraya, T. N. Blanton, Y. Wu, *J. Appl. Cryst.* **1993**, *26*, 180–184.
27. C. J. Gommes, B. Goderis, *J. Appl. Cryst.* **2010**, *43*, 352–355.
28. J. Škerjanc, K. Kogej, *J. Phys. Chem*. **1989**, *93*, 7913–7915.
29. C. Tanford, *The Hydrophobic Effect: Formation of Micelles and Biological Membrane*, John Wiley & Sons, New York, 1980.

30. R. W. Armstrong, U. P. Strauss, in: *Encyclopedia of Polymer Science and Technology*; Interscience: New York, 1968; Vol. 10.
31. M. Andersson, P. J. Rasmark, C. Elvingson, P. Hansson *Langmuir* **2005**, *21*, 3773–3781.
32. R. J. Hunter, *Foundations of Colloid Science*, Vol. 1, Clarendon Press, Oxford, 1987.

Povzetek

Študirali smo fazno obnašanje in strukture faz v sistemu natrijev polistirensulfonat, NaPSS, kompleksna sol CTAPSS (med cetiltrimetilamovijevimi kationi, CTA^+, in polistirensulfonatnim anionom, PSS), voda. Pokazali smo, da pri tvorbi agregata med poliionom in surfaktantom poleg močne elektrostatske interakcije pomembno vlogo igra hidrofobna interakcija zaradi prisotnosti stirenske skupine na poliionu. Identificirali smo le neurejeno micelno (L_1) in urejeno heksagonalno (H_1) fazo, ki sta povezani preko širokega dvofaznega področja. Pri vsebnosti vode nad 60 masnih % se CTAPSS zlahka raztopi sorazmerno z dodano količino NaPSS, pri nižjih vsebnostih vode pa je potreben velik presežek NaPSS za raztopitev kompleksne soli. Na fazno separacijo v dvofaznem področju vplivata dve tendenci: (i) težnja po čim večjem kontaktu med hidrofobnimi skupinami na PSS (kjer poglavitno vlogo igra hidrofobna interakcija) in (ii) težnja po tvorbi čim gostejše faze (kjer sta pomembni tako elektrostatska kot hidrofobna interakcija). Strukturne lastnosti kompleksov v micelni fazi kažejo, da hidrofobna interakcija prispeva k sorazmerno majhnim razdaljam med micelami, ki so vezane na PSS, in vodi do šibke asociacije med verigami PSS v obliki fizikalne mreže, kjer micele igrajo vlogo mrežnih mest.